



## Cobalt-nickel alloy catalysts for hydrosilylation of ketones synthesized by utilizing metal-organic framework as template

**Bennedsen, Niklas Rosendal; Kramer, Søren; Mielby, Jerrik Jørgen; Kegnæs, Søren**

*Published in:*  
Catalysis Science & Technology

*Link to article, DOI:*  
[10.1039/c8cy00150b](https://doi.org/10.1039/c8cy00150b)

*Publication date:*  
2018

*Document Version*  
Peer reviewed version

[Link back to DTU Orbit](#)

*Citation (APA):*  
Bennedsen, N. R., Kramer, S., Mielby, J. J., & Kegnæs, S. (2018). Cobalt-nickel alloy catalysts for hydrosilylation of ketones synthesized by utilizing metal-organic framework as template. *Catalysis Science & Technology*, 8(9), 2434-2440. <https://doi.org/10.1039/c8cy00150b>

---

### General rights

Copyright and moral rights for the publications made accessible in the public portal are retained by the authors and/or other copyright owners and it is a condition of accessing publications that users recognise and abide by the legal requirements associated with these rights.

- Users may download and print one copy of any publication from the public portal for the purpose of private study or research.
- You may not further distribute the material or use it for any profit-making activity or commercial gain
- You may freely distribute the URL identifying the publication in the public portal

If you believe that this document breaches copyright please contact us providing details, and we will remove access to the work immediately and investigate your claim.

# Catalysis Science & Technology

Accepted Manuscript



This article can be cited before page numbers have been issued, to do this please use: N. R. Bennedsen, S. Kramer, J. Mielby and S. Kegnaes, *Catal. Sci. Technol.*, 2018, DOI: 10.1039/C8CY00150B.



This is an Accepted Manuscript, which has been through the Royal Society of Chemistry peer review process and has been accepted for publication.

Accepted Manuscripts are published online shortly after acceptance, before technical editing, formatting and proof reading. Using this free service, authors can make their results available to the community, in citable form, before we publish the edited article. We will replace this Accepted Manuscript with the edited and formatted Advance Article as soon as it is available.

You can find more information about Accepted Manuscripts in the [author guidelines](#).

Please note that technical editing may introduce minor changes to the text and/or graphics, which may alter content. The journal's standard [Terms & Conditions](#) and the ethical guidelines, outlined in our [author and reviewer resource centre](#), still apply. In no event shall the Royal Society of Chemistry be held responsible for any errors or omissions in this Accepted Manuscript or any consequences arising from the use of any information it contains.



## Journal Name

## ARTICLE

Received 00th January  
20xx,

## Cobalt-nickel alloy catalysts for hydrosilylation of ketones synthesized by utilizing metal-organic framework as template

Niklas R. Bennedsen<sup>a</sup>, Søren Kramer<sup>a</sup>, Jerrik J. Mielby<sup>a</sup> and Søren Kegnæs<sup>\*a</sup>

Accepted 00th January 20xx

DOI: 10.1039/x0xx00000x

www.rsc.org/

In this article, we report an approach to synthesize alloy Co-Ni nanoparticles encapsulated in carbon by utilization of the MOF, ZIF-67, as a sacrificial template. The alloy CoNi materials are synthesized by incipient wetness impregnation of cobalt-containing ZIF-67 with nickel(II) nitrate followed by carbonization. The formation of alloy nanoparticles was verified by XRD and TEM analysis showed that they are distributed evenly throughout the entire material. The carbon encapsulating the alloy nanoparticles is N-doped and graphitic according to XPS analysis. Further characterization by ICP, N<sub>2</sub>-physisorption, and SEM imaging was also performed. The CoNi materials exhibited promising activity in the catalytic hydrosilylation of ketones. A carbonization temperature of 800 °C provided the best catalyst for this transformation. The reaction conditions were optimized, different silanes tested, a time study conducted, and the heterogeneity of the catalysis assessed with different tests. Finally, a substrate scope of various ketones was examined.

### Introduction

Metal-organic frameworks (MOFs) have attracted much attention due to their high porosity, surface area, and easily tunable chemical structure.<sup>1,2,3,4</sup> As a consequence of these features, MOFs have found applications in various fields such as chemical sensing<sup>5</sup>, gas storage<sup>6,7</sup>, photocatalysis<sup>8,9</sup> and catalysis<sup>3,10</sup>. One of the remaining challenges associated with the use of MOFs as catalysts is their often moderate thermal stability. Accordingly, as an alternative approach to catalyst synthesis, MOFs have been used as structural templates and source of carbon for the formation of metal nanoparticles encapsulated in a porous matrix.<sup>11</sup> This process is facilitated by carbonization of the MOF. In contrast to the parent MOFs (non-carbonized), these encapsulated metal nanoparticles typically possess improved chemical and thermal stability required for catalytic reactions and efficient catalyst recycling. Most of the reported studies focus on carbonization of monometallic MOFs such as the isostructural Zn<sup>2+</sup>-containing ZIF-8 and Co<sup>2+</sup>-containing ZIF-67, where the metal ions are linked by 2-methylimidazole.<sup>12,13,14</sup>

Recently, the use of catalysts consisting of metal nanoparticles which are alloys of abundant, non-noble metals has received considerable due to the intriguing properties of these materials.<sup>15,16,17</sup> Alloying non-noble metals together may achieve the desired activity and selectivity often observed by using precious metals as seen in the synthesis of ammonia with a cobalt/molybdenum alloy.<sup>18</sup> In the case of alloy nanoparticles

between cobalt and nickel, they have shown enhanced catalytic activity in CO<sub>2</sub> dry-reforming<sup>19,20</sup>, water splitting<sup>21</sup>, oxygen evolution reaction<sup>22</sup>, and H<sub>2</sub> release<sup>23</sup>. However, in terms of their use in reactions for synthetic organic chemistry, very few examples exist. Recently, our group have published that alloy CoNi nanoparticle are active catalysts for a series of organic reactions, including silylative pinacol coupling reactions and double bond migrations.<sup>24,25</sup>

In the synthesis of alloy CoNi nanoparticles, ZIF-67 is of interest due to its inherent cobalt content, which during carbonization facilitate the formation of cobalt nanoparticles encapsulated in porous N-doped carbon. These nanoparticles are ideal for heterogeneous catalysis.<sup>11,26</sup> However, only few attempts to synthesize alloy metal nanoparticles by introducing additional metals into the ZIF prior to the carbonization process are reported and no CoNi alloys accessed from ZIF-67 are reported.<sup>27</sup>

Reduction of ketones by hydrogenation or hydrosilylation is an important and widely used transformation in the production of fine chemicals, such as pharmaceuticals.<sup>28</sup> The hydrosilylation approach avoids the use of high pressures, which can be a requirement for hydrogenations. For ketone hydrosilylation, homogeneous precious metal catalysts have typically been used.<sup>29</sup> However, significant recent advances in homogeneous base metal catalysis has led to the development of highly efficient catalytic systems based on these inexpensive metals.<sup>30</sup> While selectivity and activity is often higher in homogeneous catalysis, heterogeneous catalysis offers significant advantages in terms of recyclability, ease of catalyst separation, and robustness. Thus, the development of heterogeneous base metal catalysts for hydrosilylation of ketones is of high importance. Only a few reports exist on heterogeneous base metal catalysed ketone hydrosilylation.<sup>31</sup>

<sup>a</sup> Department of Chemistry, DTU, Technical University of Denmark, DK-2800 Kgs. Lyngby, Denmark.  
skk@kemi.dtu.dk

Electronic Supplementary Information (ESI) available: [details of any supplementary information available should be included here]. See DOI: 10.1039/x0xx00000x

Herein, we report a new way to synthesize alloy cobalt-nickel alloys by the utilization of ZIF-67 as sacrificial template, and source of carbon, nitrogen, and cobalt. The porous structure of ZIF-67 facilitates the introduction of nickel into the pores by incipient wetness impregnation before carbonization. Carbonization of the impregnated ZIF-67 promotes the formation of alloy cobalt-nickel nanoparticles encapsulated in a porous carbon matrix. The synthesized alloy materials are abbreviated  $\text{CoNi@NC}_x$ , where NC is porous N-doped carbon and X represents the carbonization temperature, which was either 550, 675 or 800 °C (Figure 1). The resulting material was assessed in the hydrosilylation of ketones. The assessment involves optimization of the reaction conditions, time study, recycling experiment, ketone scope, and silane scope.

## Experimental

### Synthesis of ZIF-67<sup>1</sup>

The synthesis of ZIF-67 was adapted from David Lou *et al.*<sup>32</sup>: In short, 2.91 g (10 mmol) cobalt(II) nitrate hexahydrate ( $\text{Co}(\text{NO}_3)_2 \cdot 6\text{H}_2\text{O}$ ) and 3.28 g (40 mmol) 2-methylimidazole was dissolved separately in 250 mL MeOH. The two solutions were mixed by adding the 2-methylimidazole solution to the cobalt(II) nitrate solution. The mixture was stirred for 5 min, aged for 72 hours, collected by centrifugation, and dried in an oven overnight at 80 °C. 500 mg ZIF-67 was obtained; 23% yield based on cobalt.

### Synthesis of $\text{Co@NC}$ :

200 mg ZIF-67 was carbonized in a tube furnace at 800 °C for 3 hours with a heating ramp of 5 °C/min. This yielded 120 mg of cobalt nanoparticles encapsulated in N-doped carbon ( $\text{Co@NC}$ ) as a black powder.

### Synthesis of $\text{CoNi@NC}_x$ :

200 mg ZIF-67 (0.9 mmol cobalt) was impregnated with nickel by dissolving 262 mg (0.9 mmol)  $\text{Ni}(\text{NO}_3)_2 \cdot 6\text{H}_2\text{O}$  in 140  $\mu\text{L}$  MeOH. The resulting powder was carbonized in a tube furnace at 550, 675, or 800 °C for 3 hours with a heating ramp of 5 °C/min. This yielded 130 mg of alloyed cobalt-nickel nanoparticles encapsulated in N-doped carbon ( $\text{CoNi@NC}$ ) as a black powder.

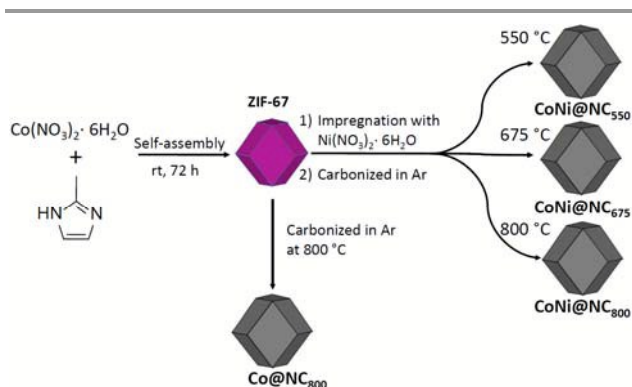


Fig. 2 Schematic overview of the different materials synthesized in this study.

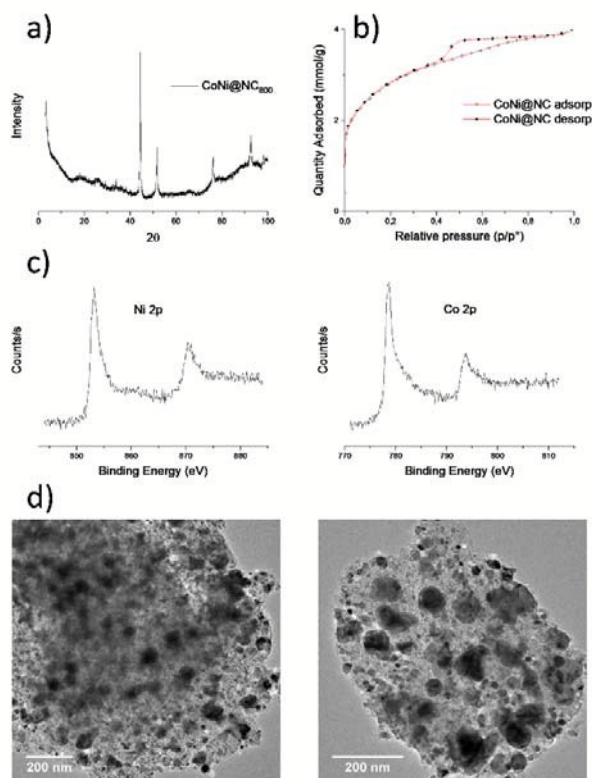


Fig. 1 Characterization of  $\text{CoNi@NC}_{800}$ . The figure includes a) XRD diffractogram, b)  $\text{N}_2$ -physorption isotherm, c) XPS analysis of Co and Ni, and d) TEM images of the catalyst.

## Results and characterization

For  $\text{CoNi@NC}_{800}$ , the XPS analysis,  $\text{N}_2$ -physorption isotherm, the X-ray diffraction (XRD) diffractogram, and TEM images of are presented in Figure 2. The characterization data for the other materials are found in supporting information. The XRD diffractogram (Figure 2a) shows that the original crystalline phase of the ZIF-67 crystals have completely converted into a carbon material. Furthermore, only one peak at  $2\theta \approx 44$  correlating to a 111-diffraction is found in the diffractogram suggesting the formation of uniform alloy nanoparticles between cobalt and nickel, and not individually monometallic nanoparticles. Additionally, the 111-diffraction peak from the alloy material is slightly shifted compared to the monometallic cobalt material, which also suggests the formation of alloy nanoparticles according to Vegard's law.<sup>33</sup> These observations are consistent with a previously reported  $\text{CoNi}$  alloy material synthesized by carbonization of a mixed metal-EDTA salt.<sup>25,34</sup> Diffractograms of the other materials are found in Figure S5.

The  $\text{N}_2$ -physorption adsorption/desorption isotherm for  $\text{CoNi@NC}_{800}$  shown in Figure 2b is best described as a mixture of type I and IV by the IUPAC nomenclature with the presence of a hysteresis indicating the mesoporous nature of the carbon material.<sup>35</sup> The estimated pore volume, microporous volume and BET surface for all the synthesized materials are summarized in Table 1. It is clear that the original pore volume,

**Table 1** Values obtained from N<sub>2</sub>-physisorption from the four different catalytic materials and the template ZIF-67.

Catalyst	Pore volume <sup>1</sup> (cm <sup>3</sup> /g)	Microporous volume <sup>2</sup> (cm <sup>3</sup> /g)	Surface area <sup>3</sup> (m <sup>2</sup> /g)
ZIF-67	0.762	0.664	1364
CoNi@NC550	0.132	0.096	232
CoNi@NC675	0.152	0.072	246
CoNi@NC800	0.135	0.024	213
Co@NC800	0.184	0.043	283

<sup>1</sup> Single point read at p/p<sub>0</sub>. <sup>2</sup> t-plot method. <sup>3</sup> BET method.

**Table 2** Catalytic activity tests for the synthesized materials.

Entry	Catalyst	Conversion (%)	Yield (%)
1	ZIF-67	3	1
2	CoNi@NC550	80	68
3	CoNi@NC675	71	62
4	CoNi@NC800	86	73
5	Co@NC800	30	3

Yield based on <sup>1</sup>H NMR using 0.5 equivalents of dibenzyl ether as standard.

microporosity and BET surface area of ZIF-67 is lost during the impregnation and carbonization process.

The different elemental species present in the carbonized materials were assessed by XPS analysis for cobalt, nickel, carbon, and nitrogen. The spectra are in the supporting information (Figure S8-11) but the 2p scan for cobalt and nickel are in Figure 2 for the CoNi@NC<sub>800</sub> catalyst. The spectra show the presence metallic Co and Ni at 779.7 eV and 852.6 eV, respectively. For the samples carbonized at 550 and 675 °C, a larger proportion of metal oxide is observed which may be caused by the presence of smaller metal nanoparticles providing more surface that can be oxidized.<sup>36</sup> Examination of the carbon present in the catalyst by XPS suggests that the majority is sp<sup>2</sup>-hybridized carbon, i.e. graphitic. This is exemplified by the 1s peak for carbon which is present at 284.8 eV where graphitic carbon is reported at 284 eV.<sup>37</sup> XPS spectra of nitrogen indicates that multiple species are present in the catalysts carbonized at 800 °C. The 1s peaks from nitrogen are present at both 399 eV and 401 eV which correlates to pyridinic nitrogen, and either pyrrolic or graphitic nitrogen or a combination of both.<sup>38</sup> As for the materials carbonized at 550 or 675 °C, the pyridinic nitrogen species are more profound. Additional investigation of the atom configuration of the CoNi@NC<sub>800</sub> catalyst is shown in Figure S8.

ICP-OES analysis of CoNi@NC<sub>800</sub> reveals that 67% of the catalyst is metal with a Co:Ni ratio of 60:40. This suggests that some of the added nickel during the incipient wetness impregnation is not incorporated into the final material.

**Table 3** Screening of different silanes conducted under optimized conditions.

Entry	HSiR <sub>3</sub>	Conversion (%)	Yield (%)
1	Me <sub>2</sub> PhSiH	100	100
2	Et <sub>3</sub> SiH	85	50
3	EtMe <sub>2</sub> SiH	100	78
4	MePh <sub>2</sub> SiH	51	36
5	Ph <sub>3</sub> SiH	11	0

Yield based on <sup>1</sup>H NMR using 0.5 equivalents of dibenzyl ether as standard.

The TEM image for the CoNi@NC<sub>800</sub> catalyst in Figure 2 shows the distribution of CoNi alloy nanoparticles throughout all of the material. However, due to the high metal content, partial particle agglomeration is occurring, which leads to a broad size distribution of metal nanoparticles ranging from 10-75 nm.

SEM images of the carbonized CoNi@NC<sub>800</sub> show that the characteristic rhombic dodecahedron shape of ZIF-67 is not preserved after the carbonization process. To analyse the origin of the structural change, carbonized ZIF-67 without the nickel impregnation step was also analysed and showed no structural change. This implies that a structural change is occurring because of the impregnation with nickel prior to the carbonization process. The SEM images are in Figure S13-14.

Initially, the different materials were compared, and the CoNi@NC<sub>800</sub> catalyst showed the most promising results (Table 2). The subsequent optimization of the reaction conditions revealed that better selectivity and complete conversion of cyclohexanone in 24 hours could be obtained in heptane with 10 mg of catalyst and only a small excess of Me<sub>2</sub>PhSiH (Table 3, entry 1). Additional information about the optimization process is presented in Table S2-3 in the supporting information.

The influence of the silane was investigated by screening five different silanes as shown in Table 3. Me<sub>2</sub>PhSiH gives the highest yield and selectivity towards the hydrosilylation product (entry 1). Other silanes show good to high activity, except the bulky Ph<sub>3</sub>SiH (entry 5). It appears that the introduction of more bulky groups to the silane decreases the activity of the hydrosilylated product by comparing entry 1, 4, and 5 (Me<sub>2</sub>PhSiH > MePh<sub>2</sub>SiH > Ph<sub>3</sub>SiH).

The time study presented in Figure 3 shows an induction period of approximately 4 hours where no catalytic activity is observed. It is also evident from the time study that 24 hours is required for a complete reaction with cyclohexanone under the optimized conditions.

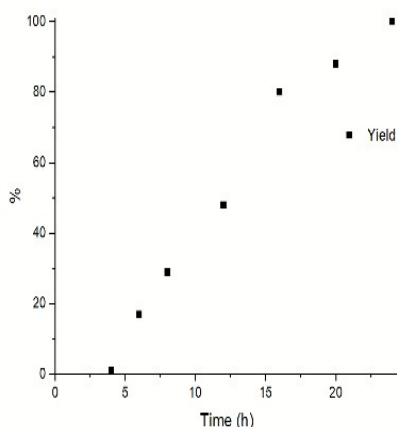


Fig. 3 Time study presented with yield as a function of reaction time. The study was conducted under optimized conditions with cyclohexanone (Table 3, entry 1).

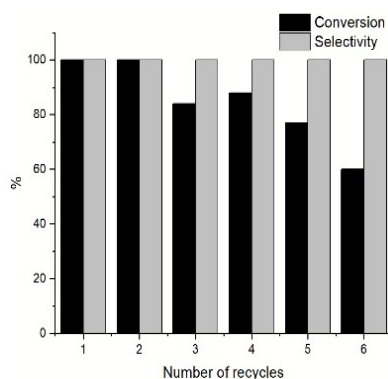
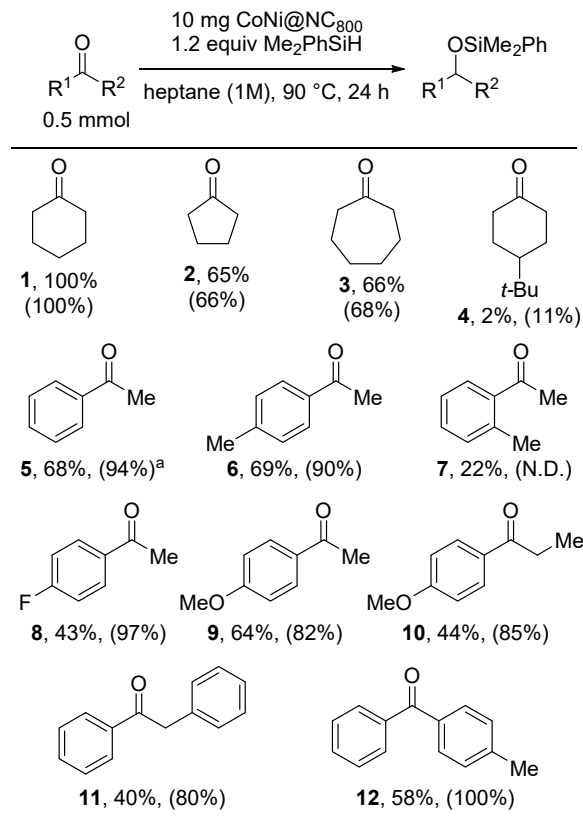


Fig. 4 The catalyst was recycled six times. The recycling of the catalyst was facilitated by separating the catalyst from the reaction mixture by a magnet, which exploited the magnetic properties of the catalyst

In order to examine the recyclability of the catalyst, seven consecutive reactions (six recycles) with the same catalyst were performed (Figure 4). The magnetic properties of the catalyst allow for easy recycling by a simple magnetic filtration. Over the course of seven reactions, the catalyst maintains 100% selectivity, but a decrease in conversion from 100% to 60% was observed. By analysing the catalyst after the seventh reaction by TEM (Figure S15), it is evident that the alloy metal nanoparticles have agglomerated which is a likely explanation for the deactivation. We also investigated the possibility of metal leaching during the reaction by ICP-OES analysis of two reaction mixtures, which were filtered after 24 hours. In both cases, the cobalt and nickel content in the filtrate was below detection limit (equal to a blank sample). Finally, a hot filtration test was performed to support the suggested heterogeneous nature of catalysis. After 12 hours of reaction, the reaction mixture was filtered while hot and filtrate kept at 90 °C for additional 8 hours. No additional conversion was observed in the filtrate, hence indicating that the catalysis is heterogeneous.

Table 4 Scope of different ketones for the hydrosilylation reaction



Yields are based on <sup>1</sup>H NMR using 0.5 equivalents dibenzyl ether as standard. Conversion of the ketone is shown in parenthesis. a) 2.0 equivalents Me<sub>2</sub>PhSiH.

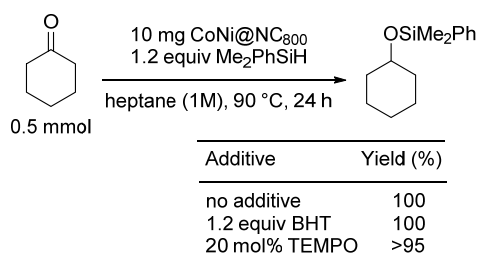
For a single reaction, the TON and TOF is 11 and 0.46 h<sup>-1</sup>, respectively.<sup>39</sup> However, taking into account the facile recycling, a summative TON of 67 is obtained after seven consecutive reactions. Albeit higher TONs can be obtained with other base metals, the obtained TON is more than three times greater than a recent report using a homogeneous nickel catalyst (at 100 °C).<sup>40</sup>

In order to examine the generality of the developed methodology, a range of ketones was subjected to the reaction conditions (Table 4). Cyclopentanone (**2**) and cycloheptanone (**3**) displayed excellent selectivity with good yields in both cases, thus demonstrating only a small influence from the ring-size. A sterically hindered *tert*-butyl-substituted cyclohexanone (**4**) led to apparent inhibition of the activity. The yield of the hydrosilylated product from acetophenone (**5**) was moderate under standard conditions but was improved by using 2.0 equivalents of Me<sub>2</sub>PhSiH instead of 1.2 equivalents. A methyl group in the *para* position of acetophenone increased activity and yield, whereas a methyl in the *ortho* position decreased activity and yield (**6-7**). *p*-Fluoroacetophenone (**8**) is very active with 97 % conversion and moderate yield of the hydrosilylated product. In contrast, the selectivity is markedly improved for *p*-methoxyacetophenone (**9**) which gives a good yield of the hydrosilylated product. However, the introduction of sterical hindrance decreases the yield and activity (**10**). A comparable

result was obtained with 2-phenylacetophenone (**11**). Finally, the diaryl ketone (**12**) provided 58% yield of the hydrosilylated product.

In a previous extensive mechanistic study, we obtained evidence for the formation of silyl radicals from HSiEt<sub>3</sub> mediated by a related NiCo@NC catalyst.<sup>24</sup> In order to test for a radical pathway with the catalyst reported here, we performed the standard reaction in the presence of the radical inhibitors BHT and TEMPO (Scheme 1). The addition of 1.2 equivalents BHT or 20 mol% TEMPO did not affect the reaction outcome. In addition, no TEMPO adducts from radical trapping was observed at the end of the reaction.<sup>41</sup> In combination with the heterogeneity tests and sensitivity to sterical hindrance, we propose that the reaction follows the Ojima mechanism<sup>42</sup>, likely with the ketone substrate coordinating to the surface of the catalyst, which can explain the sensitivity to sterical hindrance.

**Scheme 1.** The effect of radical inhibitor and scavenger on the reaction outcome.



## Conclusions

Alloy CoNi nanoparticles encapsulated in porous carbon were successfully synthesized by utilizing ZIF-67 as a sacrificial template. The synthesis was facilitated by incipient wetness impregnation of nickel(II) nitrate into the pores of ZIF-67 followed by carbonization under an argon atmosphere.

XRD confirms the presence of alloy nanoparticles, and their unique catalytic activity was highlighted by comparing the monometallic Co@NC<sub>800</sub> catalyst with the CoNi@NC<sub>x</sub> materials. The porous carbon in the catalyst is N-doped and graphitic. A structural change from the characteristic rhombic dodecahedron shape occurred as a consequence of the incorporation of nickel during the carbonization process. The alloy materials displayed good catalytic activity in the hydrosilylation of cyclohexanone. Albeit higher activities can be accessed with some homogeneous base metal catalysts, easy recycling of the developed CoNi@NC catalyst can provide TONs which surpass a comparable homogeneous nickel catalyst. For a range of ketones good-to-high yields of the hydrosilylation products were obtained. A hot filtration experiment and ICP-OES supported the heterogeneous nature of catalysis and absence of leaching. However, slow deactivation by agglomeration was observed by TEM. Finally, the reaction outcome was unaffected by the presence of radical inhibitors and we propose a surface reaction proceeding through the Ojima mechanism, i.e. without radical intermediates.

## Conflicts of interest

There are no conflicts to declare.

## Acknowledgements

This work was funded by the Independent Research Fund Denmark (Grant no. 5054-00119 and 6111-00237) by Villum Fonden (Grant No. 13158).

## Notes

<sup>1</sup>Characterization of the synthesized ZIF-67 crystals is in the supporting information.

## References

- J. L. C. Rowsell and O. M. Yaghi, *Microporous Mesoporous Mater.*, 2004, **73**, 3–14.
- C. Dey, T. Kundu, B. P. Biswal, A. Mallick and R. Banerjee, *Acta Crystallogr. Sect. B Struct. Sci. Cryst. Eng. Mater.*, 2014, **70**, 3–10.
- J. Lee, O. K. Farha, J. Roberts, K. A. Scheidt, S. T. Nguyen and J. T. Hupp, *Chem. Soc. Rev.*, 2009, **38**, 1450.
- H. Furukawa, K. E. Cordova, M. O’Keeffe and O. M. Yaghi, *Science*, 2013, **341**, 1230444–1230444.
- R. Li, X. Ren, H. Ma, X. Feng, Z. Lin, X. Li, C. Hu and B. Wang, *J. Mater. Chem. A*, 2014, **2**, 5724–5729.
- J. Qian, F. Sun and L. Qin, *Mater. Lett.*, 2012, **82**, 220–223.
- O. M. Banerjee, Rahul, Phan, Anh, Wang, Bo, Knobler, Carolyn, Furukawa Hiroyasu, O’Keeffe, Michael, Yaghi, *ReVision*, 2008, **319**, 939–943.
- H. Yang, X.-W. He, F. Wang, Y. Kang and J. Zhang, *J. Mater. Chem.*, 2012, **22**, 21849.
- A. Schejn, A. Aboulaich, L. Balan, V. Falk, J. Lalevée, G. Medjahdi, L. Aranda, K. Mozet and R. Schneider, *Catal. Sci. Technol.*, 2014, **5**, 1829–1839.
- F. Zhang, Y. Wei, X. Wu, H. Jiang, W. Wang and H. Li, *J. Am. Chem. Soc.*, 2014, **136**, 13963–13966.
- Y. V. Kaneti, J. Tang, R. R. Salunkhe, X. Jiang, A. Yu, K. C. W. Wu and Y. Yamauchi, *Adv. Mater.*, 2017, **29**, 1604898.
- Y. Z. Chen, C. Wang, Z. Y. Wu, Y. Xiong, Q. Xu, S. H. Yu and H. L. Jiang, *Adv. Mater.*, 2015, **27**, 5010–5016.
- Q. Shi, Z. Chen, Z. Song, J. Li and J. Dong, *Angew. Chem., Int. Ed.*, 2011, **50**, 672–675.
- J. Tang, R. R. Salunkhe, H. Zhang, V. Malgras, T. Ahamad, S. M. Alshehri, N. Kobayashi, S. Tominaka, Y. Ide, J. H. Kim and Y. Yamauchi, *Sci. Rep.*, 2016, **6**, 30295.
- R. Ferrando, J. Jellinek and R. L. Johnston, *Chem. Rev.*, 2008, **108**, 845–910.
- A. K. Rovik, S. K. Klitgaard, S. Dahl, C. H. Christensen and I. Chorkendorff, *Appl. Catal. A Gen.*, 2009, **358**, 269–278.
- J. Greeley and M. Mavrikakis, *Nat. Mater.*, 2004, **3**, 810–815.
- C. J. H. Jacobsen, S. Dahl, B. G. S. Clausen, S. Bahn, A. Logadottir and J. K. Nørskov, *J. Am. Chem. Soc.*, 2001, **123**, 8404–8405.
- H. Wu, H. Liu, W. Yang and D. He, *Catal. Sci. Technol.*, 2016, **6**, 5631–5646.
- K. Takanebe, K. Nagaoka, K. Nariai and K. Aika, *J. Catal.*, 2005, **232**, 268–275.
- T. V. Vineesh, S. Mubarak, M. G. Hahm, V. Prabu, S. Alwarappan and T. N. Narayanan, *Sci. Rep.*, 2016, **6**, 31202.
- J. Yu, Y. Zhong, W. Zhou and Z. Shao, *J. Power Sources*, 2017, **338**, 26–33.

- 23 B. H. Liu, Z. P. Li and S. Suda, *J. Alloys Compd.*, 2006, **415**, 288–293.
- 24 S. Kramer, F. Hejjo, K. H. Rasmussen and S. Kegnæs, *ACS Catal.*, 2017, **8**, 754–759.
- 25 S. Kramer, J. Mielby, K. Buss, T. Kasama and S. Kegnæs, *ChemCatChem*, 2017, **9**, 2930–2934.
- 26 L. He, F. Weniger, H. Neumann and M. Beller, *Angew. Chem., Int. Ed.*, 2016, **55**, 12582–12594.
- 27 X. Shi, H. Song, A. Li, X. Chen, J. Zhou and Z. Ma, *J. Mater. Chem. A*, 2017, **5**, 5873–5879.
- 28 (a) H. Nishiyama, *Transition Metals for Organic Synthesis*; M. Beller, C. Bolm, Eds.; Wiley-VCH: Weinheim, 2004; (b) L. C. Wilkins and R. L. Melen, *Coord. Chem. Rev.*, 2016, **324**, 123–139.
- 29 (a) J. Fuchs, H. F. T. Klare and M. Oestreich, *ACS Catal.* 2017, **7**, 8338–8342; (b) T. T. Metsänen, P. Hrobárik, H. F. T. Klare, M. Kaupp and M. Oestreich, *J. Am. Chem. Soc.* 2014, **136**, 6912–6915; (c) K. Riener, M. P. Högerl, P. Gigler and F. E. Kühn, *ACS Catal.*, 2012, **2**, 613–621; (d) R. J. P. Corriu and J. J. E. Moreau, *J. Chem. Soc., Chem. Commun.* 1973, 38–39; (e) I. Ojima, M. Nihonyanagi and Y. Nagai, *J. Chem. Soc. Chem. Commun.*, 1972, 938a; (f) K. Yamamoto, T. Hayashi and M. Kumada, *J. Organomet. Chem.* 1972, **46**, C65–C67.
- 30 For examples of ketone hydrosilylation catalyzed by homogeneous base-metal complexes, see: (a) T. K. Mukhopadhyay, C. L. Rock, M. Hong, D. C. Ashley, T. L. Groy, M.-H. Baik and R. J. Trovitch, *J. Am. Chem. Soc.* 2017, **139**, 4901–4915; (b) T. Bleith and L. H. Gade, *J. Am. Chem. Soc.* 2016, **138**, 4972–4983; (c) W. Zhou, S. L. Marquard, M. W. Bezpalko, B. M. Foxman and C. M. Thomas, *Organometallics* 2013, **32**, 1766–1772; (d) ; (e) A. Albright and R. E. Gawley, *J. Am. Chem. Soc.* 2011, **133**, 19680–19683; (f) S. Chakraborty, J. A. Krause and H. Guan, *Organometallics* 2009, **28**, 582–586; (g) A. M. Tondreau, J. M. Darmon, B. M. Wile, S. K. Floyd, E. Lobkovsky and P. Chirik, *Organometallics* 2009, **28**, 3928–3940; (h) A. M. Tondreau, E. Lobkovsky and P. Chirik, *Org. Lett.* 2008, **10**, 2789–2792; (i) J. K. Kassube, H. Wadepohl and L. H. Gade, *Adv. Synth. Catal.* 2008, **350**, 1155–1162; (j) S. Rendler and M. Oestreich, *Angew. Chem. Int. Ed.* 2007, **46**, 498–504; (k) J. Yun and S. L. Buchwald, *J. Am. Chem. Soc.* 1999, **121**, 5640–5444; (l) H. Mimoun, J. Y. de Saint Laumer, L. Giannini, R. Scopelliti and C. Floriani, *J. Am. Chem. Soc.* 1999, **121**, 6158–6166.
- 31 (a) M. Li, B. Li, H.-F. Xia, D. Ye, J. Wu and Y. Shi, *Green. Chem.* 2014, **16**, 2680–2688; (b) M. L. Kantam, S. Laha, J. Yadav, P. R. Likhari, B. Sreedhar and B. M. Choudary, *Adv. Synth. Catal.* 2007, **349**, 1797–1802; (c) B. H. Lipshutz, B. A. Frieman and A. E. Tomaso Jr., *Angew. Chem. Int. Ed.* 2006, **45**, 1259–1264.
- 32 H. Hu, B. Guan, B. Xia and X. W. Lou, *J. Am. Chem. Soc.*, 2015, **137**, 5590–5595.
- 33 N. W. Denton, A R, Ashcroft, 1991, **43**, 3161–3164.
- 34 J. Deng, P. Ren, D. Deng and X. Bao, *Angew. Chem., Int. Ed.*, 2015, **54**, 2100–2104.
- 35 M. Thommes, K. Kaneko, A. V. Neimark, J. P. Olivier, F. Rodriguez-Reinoso, J. Rouquerol and K. S. W. Sing, *Pure Appl. Chem.*, 2015, **87**, 1051–1069.
- 36 F. Goodarzi, L. Kang, F. R. Wang, F. Joensen, S. Kegnæs and J. Mielby, *ChemCatChem*, , DOI:10.1002/cctc.201701946.
- 37 Y. Wang, C. Wang, Y. Wang, H. Liu and Z. Huang, *J. Mater. Chem. A*, 2016, **4**, 5428–5435.
- 38 J. Zhang, Z. Xia and L. Dai, *Sci. Adv.*, 2015, **1**, e1500564.
- 39 While cobalt is necessary for the material synthesis, nickel appears to be the active metal for the hydrosilylation (Table 2, entry 5). Accordingly, the TON and TOF is based on the nickel content of the catalyst material.
- 40 J. Zheng, C. Darcel, and J.-B. Sortais, *Catal. Sci. Technol.* 2013, **3**, 81–84.
- 41 An  $\alpha$ -cyclopropyl ketone (cyclopropyl 4-methoxyphenyl ketone) was also explored as a possible radical trap; however, this substrate was unreactive under the optimized reaction conditions, possibly due to sterical hindrance.
- 42 (a) C. Reyes, A. Prock and W. P. Giering, *Organometallics* 2002, **21**, 546–554; (b) I. Ojima, M. Nihonyanagi, T. Kogure, M. Kumagai, S. Horiuchi, K. Nakatsugawa and Y. Nagai, *J. Organometal. Chem.* 1975, **94**, 449–461.



The facile synthesis of CoNi@NC materials from a MOF precursor is reported along with the catalytic properties in ketone hydrosilylation

